Materials Physics and Mechanics 18 (2013) 108-126 Received: November 26, 2013

ON FRACTIONAL ULTRA-LASER TWO-STEP THERMOELASTICITY

Magdy A. Ezzat[1*], Ahmed S. El-Karamany[2], A.A. El-Bary[3], Mohsen A. Fayik[1]

[1] Department of Mathematics, Faculty of Education, Alexandria University, Alexandria, Egypt

[2]Department of Mathematical and Physical Sciences, Nizwa University, Nizwa -611, P. O. Box 1357, Oman

[3]Arab Academy for Science and Technology, P.O. Box 1029, Alexandria, Egypt

*e-mail: maezzat2000@yahoo.com

Abstract. In this work, a new mathematical model of two-step heat conduction for an isotropic generalized thermoelasticity is derived using the methodology of fractional calculus. Some theorems of generalized thermoelasticity follow as limiting cases. An ultrafast fractional thermoelasticity model utilizing the modified fractional parabolic two-step heat conduction model and the generalized fractional thermoelastic theory was formulated to describe the thermoelastic behavior of a thin metal irradiated by a femtosecond laser pulse. The temporal profile of the ultrafast laser was regarded as being non-Gaussian. An analytical–numerical technique based on the Laplace transform was used to solve the governing equations and the time histories of the electron temperature, lattice temperature, displacement and stress in gold were analyzed. Some comparisons have been shown in figures to estimate the effects of the fractional order parameter on all the studied fields. The effect of α where $(0<\alpha<1)$, on all the fields is very much prominent, as the calculation results show that an ultrafast laser pulse at $\alpha=1$, induces a stronger stress wave and stronger stress attenuation compared with fractional α. In addition, the peak values of the electron, lattice temperatures and the displacement are larger in a modified fractional model as compared with the original model $(\alpha=1)$. Thus, we can draw the conclusion that an ultrafast laser pulse induces a stronger thermo-mechanical response in a modified fractional model.

Nomenclature

α	fractional derivative order;
θ	non-dimensional temperature;
l	lattice;
λ	Lamé constant;
μ	shear modulus;
ρ	mass density;
τ	relaxation time;
Λ	electron mean free path;
C	volumetric heat capacities;
L	dimensional material thickness;
S	energy source of the laser pulse;
t	time;
T	absolute temperature;
R	rejectivity of the irradiated surface;
u	lattice displacement;

v speed of sound;
x one-dimensional space variable;
α_T thermal expansion coefficient;
μ_F Fermi energy;
υ_F Fermi velocity;
σ_{ij} components of stress tensor;
e_{ij} components of strain tensor;
k_B Boltzmann's constant;
k_e thermal conductivity of the electrons;
k_{eq} thermal conductivity of the electron;
n_e density of free electrons per unit volume;
J_0 total power carried by the pulse per unit cross section of the beam;
t_p time duration of the laser pulse;
T_D Debye temperature;
T_0 ambient temperature;
x_0 absorptive depth of the heat energy.

Subscript
e electron;
p pulse;
0 room temperature (300 K) or reference state.

1. Introduction

When the laser pulse duration is on the order of or shorter than the electron-photon thermalization time (picoseconds for metals), laser material interaction is a two-step, non-equilibrium heating process [1]. In the first step, the incident laser energy is absorbed predominantly by electrons during the photon excitation. In the second step, a portion of the electron thermal energy transfers to the neighboring phonon (lattice) through electron-phonon coupling. Meanwhile, a part of the electron thermal energy diffuses, through electrons, into the deeper region of electrons [2].

Researchers have proposed several models to describe the mechanism of heat conduction during short-pulse laser heating, such as the parabolic one-step model [3], the hyperbolic one-step model [4], the parabolic two-step and hyperbolic two-step models [5]. It has been found that usually the microscopic two-step models (parabolic and hyperbolic two-step models) are useful for modification material as thin films [6-8].

Differential equations of fractional order have been the focus of many studies due to their frequent appearance in various applications in fluid mechanics, viscoelasticity, biology, physics and engineering. The most important advantage of using fractional differential equations in these and other applications is their non-local property. It is well known that the integer order differential operator is a local operator but the fractional order differential operator is non-local. This means that the next state of a system depends not only upon its current state but also upon all of its historical states. This is more realistic and it is one reason why fractional calculus has become more and more popular [9-11].

Although the tools of fractional calculus were available and applicable to various fields of study, the investigation of the theory of fractional differential equations was initiated quite recently by Caputo [9]. The differential equations involving Riemann–Liouville differential

operators of fractional order $0 < \alpha < 1$, appear to be important in modeling several physical phenomena and therefore seem to deserve an independent study of their theory parallel to the well-known theory of ordinary differential equations

Fractional calculus has been used successfully to modify many existing models of physical processes. One can state that the whole theory of fractional derivatives and integrals was established in the 2nd half of the 19^{th} century. The first application of fractional derivatives was given by Abel who applied fractional calculus in the solution of an integral equation that arises in the formulation of the Tautochrone problem. The generalization of the concept of derivative and integral to a non-integer order has been subjected to several approaches and some various alternative definitions of fractional derivatives appeared in [12-16]. In the last few years fractional calculus was applied successfully in various areas to modify many existing models of physical processes, e.g., chemistry, biology, modeling and identification, electronics, wave propagation and viscoelasticity [17-20]. Fractional order models often work well, particularly for dielectrics and viscoelastic materials over extended ranges of time and frequency [21, 22]. In heat transfer and electrochemistry, for example, the half order fractional integral is the natural integral operator connecting the applied gradients (thermal or material) with the diffusion of ions of heat [23, 24]. One can refer to Padlubny [10] for a survey of applications of fractional calculus.

A quasi-static uncoupled theory of thermoelasticity based on fractional heat conduction equation was put forward by Povstenko [25]. The theory of thermal stresses based on the heat conduction equation with the Caputo time-fractional derivative, is used by Povstenko [26] to investigate thermal stresses in an infinite body with a circular cylindrical hole. Sherief et al. [27] introduced a new model of thermoelasticity using fractional calculus, proved a uniqueness theorem, and derived a reciprocal relation and a variational principle. Youssef [28] introduced another new model of fractional heat conduction equation, proved a uniqueness theorem and presented one-dimensional applications. The first writer [29, 30] established a new model of fractional heat conduction equation by using the new Taylor series expansion of time-fractional order which developed by Jumarie [31]. The reciprocity relation in case of quiescent initial state is found to be independent of the order of differintegration [32] and [33]. Ezzat and Fayik [34] studied the thermoelastic diffusion problem with one relaxation time. Ezzat and El-Karamany [35, 36] solved some problems in a perfect conducting thermoelastic medium with fractional order heat transfer. The state space approach was used to obtain the solution [37].

The current manuscript is an attempt to derive a new theory of thermoelasticity with two step heat conduction using the methodology of the fractional calculus theory. There are many models that have been reached as special cases of the new mathematical model. The fractional thermoelastic characteristics in a metal irradiated by a femtosecond laser pulse with a non-Gaussian temporal profile are investigated. The modified two-step heat conduction model and the coupling between the strain rate and the lattice temperature are considered. An analytical-numerical technique based on the Laplace transform is used to solve the governing equations [38]. Numerical results for electron temperature, lattice temperature, displacement and stress in the physical space-time domain have been obtained for a gold thin material and presented graphically. Some comparisons have been shown in figures to estimate the effect fractional order parameter on all studied fields.

2. The mathematical model for fractional two-step heat model

During laser-metal interaction, the laser energy is first deposited into electrons on metal surface, where two competing processes occur [39]. One is ballistic motion of the excited electrons into deeper parts of the metal with velocities close to the Fermi velocity ($\sim 10^6$ m/s). Another is a collision between the excited electrons and electrons around the Fermi level –

an electron temperature is defined upon establishment of equilibrium among hot electrons. These hot electrons are then diffused into deeper parts of the electron gas at a speed ($<10^4$ m/s) much lower than that of the ballistic motion. Meanwhile, the hot electrons are cooled by transferring their energy to the lattice through electron-phonon coupling. The nonequilibrium between electrons and lattice has been observed experimentally [40, 41] and can be described by the two-temperature model, which was originally proposed by Anisimov et al. [1] and rigorously derived by Qiu and Tien [5] from the Boltzmann transport equation.

Assuming heat conduction in the electron can be described by modified fractional Fourier's law and neglecting heat conduction in the lattice, the energy equations of the free electrons and lattices (phonons) are

$$C_e \frac{\partial T_e}{\partial t} = \nabla \cdot (k_e \nabla T_e) - G(T_e - T_l) + S \ , \tag{1}$$

$$C_l \frac{\partial T_l}{\partial t} = G(T_e - T_l) , \tag{2}$$

where

$$\begin{cases} C_l = \rho C_e , \\ C_e = \dfrac{\pi^2 n_e k_B}{2\mu_F} T_e = B_e T_e . \end{cases} \tag{3}$$

Equation (3) indicates that the volumetric heat capacity of the electron is proportional to the electron temperature. It should be noted that the volumetric heat capacity of electrons is much less than that of the lattice even at very high electron temperature.

On nonequilibrium condition, thermal conductivity of the electrons depends on the temperatures of both electron and lattice, hence

$$k_e = k_{eq}\left(\frac{T_e}{T_l}\right), \tag{4}$$

where $k_{eq}(T)$ is the thermal conductivity of the electron when the electrons and lattice are in thermal equilibrium. The electron-lattice coupling factor *G*, is to account for the rate of energy exchange between electrons and phonons and it can be estimated by

$$G = \frac{9}{16}\frac{n_e k_B^2 T_D^2 \upsilon_F}{\Lambda(T_l) T_l \mu_F} . \tag{5}$$

Neglecting conduction in the lattice is justified by the fact that the thermal conductivity of the lattice is two orders of magnitude smaller than that of the free electrons [42]. The heat conduction model represented by Eqs. (1) and (2) is referred to as a parabolic two-step model because Fourier's law was used to describe heat transfer in the electron gas.

Assuming all properties of electrons and lattice are independent from temperatures, one can obtain a single energy equation for lattice temperature by combining Eqs. (1) and (2). Solving for T_e from Eq. (2) yields

$$T_e = T_l + \frac{C_l}{G}\frac{\partial T_l}{\partial t} . \tag{6}$$

Substituting Eq. (6) into Eq. (1), we have

$$C_e \frac{\partial}{\partial t}\left(T_l + \frac{C_l}{G}\frac{\partial T_l}{\partial t}\right) = k_e \nabla^2 (T_l + \frac{C_l}{G}\frac{\partial T_l}{\partial t}) - G(\frac{C_l}{G}\frac{\partial T_l}{\partial t}) + S, \tag{7}$$

which can be rearranged as

$$\frac{C_e + C_l}{k_e}\frac{\partial T_l}{\partial t} + \frac{C_e C_l}{G k_e}\frac{\partial^2 T_l}{\partial t^2} = \nabla^2 T_l + \frac{C_l}{G}\frac{\partial T_l}{\partial t} + \frac{S}{k_e}, \tag{8}$$

where the subscript *l* for lattice has been dropped.

Comparing Eq. (8) with the energy equation for the from dual-phase lag model:

$$\frac{1}{\alpha}\left(\frac{\partial}{\partial t} + \tau_q \frac{\partial^2}{\partial t^2}\right)T = \left(1 + \tau_T \frac{\partial}{\partial t}\right)\nabla^2 T + \frac{1}{k}\left(1 + \tau_q \frac{\partial}{\partial t}\right)S. \tag{9}$$

It is apparent that they have almost identical form except the partial derivative of the heat source with respective to time is not present in Eq. (8). The thermo physical properties in the dual-phase lag model are related to the properties appearing in the two-temperature model by

$$k = k_e, \quad \alpha = \frac{k_e}{C_e + C_l}, \quad \tau_T = \frac{C_l}{G}, \quad \tau_q = \frac{C_e C_l}{G(C_e + C_l)}.$$

The ratio of two phase-lag times is

$$\frac{\tau_T}{\tau_q} = \frac{(C_e + C_l)}{C_e} = 1 + \frac{C_l}{C_e}. \tag{10}$$

which indicates that τ_T is always greater than τ_q.

2.1. Fractional hyperbolic two-step model.

If we consider the hyperbolic effect on the conduction in the electron gas, the energy equation for the electron gas is

$$C_e \frac{\partial T_e}{\partial t} = -\nabla \cdot q_e - G(T_e - T_l) + S, \tag{11}$$

and the generalized Spitzer-Harm heat-flow's law [43-44] is

$$(q_e + \tau_e \frac{\partial q_e}{\partial t}) = -k_e \nabla T_e$$

The constant k_e is known as the Spitzer thermal conductivity.

Applying the new fractional Taylor's series of time-fractional order α [31] to expand $q_e(x_i, t + \tau_e)$ and retaining the term up to α-order in the thermal relaxation time τ_e, one obtains

$$q_e(x, t + \tau_e) = \left(1 + \frac{\tau_e^\alpha}{\alpha!}\frac{\partial^\alpha}{\partial t^\alpha}\right)q_e(x, t), \quad 0 < \alpha \le 1, \tag{12}$$

where $\tau_e << 1$ is the thermal relaxation time for the electron gas.

While the energy equation for the lattice is still Eq. (2). Equations (11) and (12) can be combined to yield

$$C_e\left(1+\frac{\tau_e^\alpha}{\alpha!}\frac{\partial^\alpha}{\partial t^\alpha}\right)\left[\frac{\partial T_e}{\partial t}+G(T_e-T_l)-S\right]=\nabla\cdot\left(k_e\nabla T_e\right) \tag{13}$$

The conduction model represented by Eqs. (2) and (13) is referred to as a fractional hyperbolic two-step model.

Dual-parabolic two-step model.

The contribution of heat conduction in phonons was neglected in the above two models. If it is assumed that the heat conduction in the phonons can be modeled using the classical Spitzer-Harm law, the energy equations of the lattices (phonons) are

$$C_l\frac{\partial T_l}{\partial t}=\nabla\cdot\left(k_l\nabla T_l\right)-G(T_e-T_l). \tag{14}$$

The bulk thermal conductivity of metal measured at equilibrium k_{eq} is the sum of electron thermal conductivity k_e and the lattice thermal conductivity k_l. Since the mechanism for heat conduction in metal is a diffusion of free electrons, k_e is usually dominant. For gold, k_e is $99\ \%$ of k_{eq} while k_l only contributes to $1\ \%$ of k_{eq} [42].

2.2. Fractional dual-hyperbolic two-step model.

In the case that heat conduction in both electrons and photons needs to be considered using the hyperbolic model, the energy equation for the lattice becomes

$$C_l\frac{\partial T_l}{\partial t}=-\nabla\cdot q_l+G(T_e-T_l), \tag{15}$$

and the fractional Spitzer-Harm's law is

$$\left(1+\frac{\tau_l^\alpha}{\alpha!}\frac{\partial^\alpha}{\partial t^\alpha}\right)q_l(x,t)=-k_l\nabla T_l,\quad 0<\alpha\le 1, \tag{16}$$

where $\tau_l<<1$ is the thermal relaxation time of the lattices (phonons).

Combining (11) and (12) to eliminate q_l yield

$$C_l\left(1+\frac{\tau_l^\alpha}{\alpha!}\frac{\partial^\alpha}{\partial t^\alpha}\right)\left[\frac{\partial T_l}{\partial t}-G(T_e-T_l)\right]=\nabla\cdot\left(k_l\nabla T_l\right). \tag{7}$$

Equation (17) together with Eq. (13) are the governing equations for the fractional dual-hyperbolic two-step model.

3. Application

In this section, the solution for the ultrafast laser-induced thermomechanical response an ultrafast thermoelasticity model, utilizing the fractional parabolic two-step heat conduction model and the generalized thermoelastic theory is formulated. Consider an isotropic thermo elastic material such as gold with a thickness (L) under local irradiation of the front surface of a metal by a laser pulse with a non Gaussian temporal profile. This problem can be treated as a one-dimensional problem when the size of the spot irradiated and the lateral dimensions of the material are much larger than the material thickness.

Hence, the governing equations of ultrafast thermomechanical response for a homogeneous, isotropic and fractional thermoelastic medium is given

1. The uni-axial strain:

$$\varepsilon_{xx} = \frac{\partial u}{\partial x}, \tag{18}$$

where u is the lattice displacement. Thus the lattice dilatation e is obtained as

$$e = \varepsilon_{xx} = \frac{\partial u}{\partial x}. \tag{19}$$

2. The constitutive equation:

$$\sigma_{xx} = (\lambda + 2\mu)\varepsilon_{xx} - (3\lambda + 2\mu)\alpha_T (T_l - T_0). \tag{20}$$

3. Equation of motion:

$$\rho \frac{\partial^2 u}{\partial t^2} - (\lambda + 2\mu)\frac{\partial^2 u}{\partial x^2} + (3\lambda + 2\mu)\alpha_T \frac{\partial T_l}{\partial x} = 0. \tag{21}$$

4. The modified fractional parabolic two-step model which can be described by the following equations:

$$k_e T_{e,xx} - \left(1 + \frac{\tau_e^{\alpha}}{\alpha!}\frac{\partial^{\alpha}}{\partial t^{\alpha}}\right)\left[C_e \frac{\partial T_e}{\partial t} + G(T_e - T_l) - S(x,t)\right] = 0, \tag{22.a}$$

$$C_l \frac{\partial T_l}{\partial t} - G(T_e - T_l) + (3\lambda + 2\mu)\alpha_T T_l \dot{\varepsilon}_{xx} = 0. \tag{22.b}$$

5. The coupling factor between the electrons and the lattice [6]:

$$G = \frac{9}{16}\frac{n_e k_B^2 T_D^2 \upsilon_F}{\Lambda(T_l) T_l \mu_F}. \tag{23}$$

6. The temporal profile of the laser pulse is non-Gaussian and given by the following:

$$J(t) = \frac{J_0 t}{t_p^2}\exp\left(-\frac{t}{t_p}\right). \tag{24}$$

7. The thermal conduction in the beam with an energy source $S(x,t)$ is given by [45]:

$$S(x,t) = \frac{(1-R)}{x_0}\exp\left(-\frac{x}{x_0}\right)J(t). \tag{25}$$

Introducing the non-dimensional parameters:

$$x' = \frac{x}{x_0},\ u' = \frac{u}{x_0},\ t' = \frac{Gt}{C_e},\ t_p' = \frac{Gt_p}{C_e},\ \tau_e' = \frac{Gt}{C_e}\tau_e,\ \theta_e' = \frac{(T_e - T_0)}{T_0},\ \theta_l' = \frac{(T_l - T_0)}{T_0}.$$

Equations (20)-(22) can be transformed into the following dimensionless form

$$\left(1 + \frac{\tau_e^{\alpha}}{\alpha!}\frac{\partial^{\alpha}}{\partial t^{\alpha}}\right)\left[\frac{\partial \theta_e}{\partial t} + (\theta_e - \theta_l) - \Omega_2 \exp\left(-x - \frac{t}{t_p}\right)\right] = \Omega_1 \frac{\partial^2 \theta_e}{\partial x^2}, \tag{26}$$

$$\frac{\partial \theta_l}{\partial t} - \Omega_3 \frac{\partial^2 u}{\partial x \, \partial t} - \Omega_4 (\theta_e - \theta_l) = 0, \tag{27}$$

$$\frac{\partial^2 u}{\partial t^2} - \Omega_5 \frac{\partial^2 u}{\partial x^2} + \Omega_6 \frac{\partial \theta_l}{\partial x} = 0, \tag{28}$$

$$\sigma_{xx} = (\lambda + 2\mu) \frac{\partial u}{\partial x} - \Omega_3 T_0 C_l \theta_l, \tag{29}$$

where

$$\Omega_1 = \frac{k_e}{G x_0^2}, \ \Omega_2 = \frac{(1-R) J_0 C_e}{x_0 T_0 G^2}, \ \Omega_3 = \frac{\alpha_T}{C_l} (3\lambda + 2\mu), \ \Omega_4 = \frac{C_e}{C_l}, \ \Omega_5 = \frac{(\lambda + 2\mu) C_e^2}{\rho G^2 x_0^2},$$

$$\Omega_6 = \frac{(3\lambda + 2\mu) C_e^2 \alpha_T T_0}{\rho G^2 x_0^2}.$$

The governing equations are solved under proper initial and boundary conditions. For simplicity, we considered here that the material is initially unstrained, unstressed and at temperature T_0 throughout. Thus, one has the following initial conditions:

$$\theta_e(x,t)\big|_{t=0} = 0, \quad \theta_l(x,t)\big|_{t=0} = 0, \tag{30}$$

$$u(x,t)\big|_{t=0} = 0, \quad \frac{\partial u}{\partial t}(x,t)\bigg|_{t=0} = 0, \tag{31}$$

and

$$\sigma_{xx}(x,t)\big|_{t=0} = 0. \tag{32}$$

From Eqs. (30) and (32), we have

$$\frac{\partial u}{\partial x}(x,t)\bigg|_{t=0} = 0. \tag{33}$$

For the boundary conditions, assume that the thin material is attached to a rigid substrate with constant temperature (namely the ambient temperature). Heat losses to the front surface is assumed to be negligible during the ultra-short laser heating process, implying that

$$\frac{\partial \theta_l}{\partial x}\bigg|_{x=0} = 0. \tag{34}$$

The back surface is assumed to be isothermal [45, 46], that is

$$\theta_l\big|_{x=a} = 0, \tag{35}$$

where $a = L / x_0$ is the dimensionless thickness.

The front surface of the material is stress free and the back surface is fixed. That is

$$\left((\lambda + 2\mu) \frac{\partial u}{\partial x} - \Omega_3 T_0 C_l \theta_l \right)\bigg|_{x=0} = 0, \tag{36}$$

and

$$u(x,t)\big|_{x=a} = 0. \tag{37}$$

Applying the Laplace transform rule with the Caputo derivative (see Appendix (C)) for both sides of Eqs. (26)-(29), we arrive at the following set of equations

$$s\bar{\theta}_e - \alpha^* \frac{\partial^2 \bar{\theta}_e}{\partial x^2} + (\bar{\theta}_e - \bar{\theta}_l) = \beta \exp(-x), \tag{38}$$

$$s\bar{\theta}_l - s\,\Omega_3 \frac{\partial \bar{u}}{\partial x} + \Omega_4(\bar{\theta}_e - \bar{\theta}_l) = 0, \tag{39}$$

$$s^2\bar{u} - \Omega_5 \frac{\partial^2 \bar{u}}{\partial x^2} + \Omega_6 \frac{\partial \bar{\theta}_l}{\partial x} = 0, \tag{40}$$

$$\bar{\sigma}_{xx} = (\lambda + 2\mu)\frac{\partial \bar{u}}{\partial x} - \Omega_3 T_0 \bar{\theta}_l, \tag{41}$$

where

$$\alpha^* = \frac{k_e}{G(1+(\tau_0^\alpha/\alpha!)s^\alpha)x_0^2},\ \beta = \frac{\Omega_2 t_p}{(1+st_p)}.$$

From Eq. (39), we can get

$$\bar{\theta}_e = \frac{1}{\Omega_4}\left[(s+\Omega_4)\bar{\theta}_l + s\,\Omega_3 \frac{\partial \bar{u}}{\partial x}\right]. \tag{42}$$

Substitution of Eq. (42) into Eq. (38) gives

$$s(s+\Omega_4+1)\bar{\theta}_l - \alpha^*(s+\Omega_4)\frac{\partial^2 \bar{\theta}_l}{\partial x^2} + s(s+1)\Omega_3 \frac{\partial \bar{u}}{\partial x} - s\alpha^*\Omega_3 \frac{\partial^3 \bar{u}}{\partial x^3} = \beta\Omega_4 \exp(-x). \tag{43}$$

Elimination of $(\partial\bar{\theta}_l/\partial x)$ and $(\partial^2\bar{\theta}_l/\partial x^2)$ from Eqs. (40) and (43) results in

$$\bar{\theta}_l = \frac{1}{\omega_1}\left[\omega_2 \frac{\partial^3 \bar{u}}{\partial x^3} - \omega_3 \frac{\partial \bar{u}}{\partial x} + \omega_4 \exp(-x)\right], \tag{44}$$

where

$$\omega_1 = s(s+\Omega_4+1),\ \omega_2 = \alpha^*\left[\frac{\Omega_5(s+\Omega_4)}{\Omega_6} + \Omega_3 s\right],\ \omega_3 = \left[\frac{\alpha^* s^2(s+\Omega_4)}{\Omega_6} + \Omega_3 s(s+1)\right],\ \omega_4 = \Omega_4\beta.$$

Substituting Eq. (44) into Eq. (40) gives the following differential equation for $\bar{u}$:

$$\Lambda_1 \frac{\partial^4 \bar{u}}{\partial x^4} - \Lambda_2 \frac{\partial^2 \bar{u}}{\partial x^2} + \Lambda_3 \bar{u} = \Lambda_4 \exp(-x), \tag{45}$$

where the parameters $\lambda_i,\ i = 1,2,3,4$ are given in Appendix (A).

The solution of Eq. (45) is

$$\bar{u}(x,s)=\sum_{i=1}^{4}C_i\exp(\lambda_i x)+D_1\exp(-x), \tag{46}$$

Substituting Eq. (46) into Eq. (44) gives

$$\bar{\theta}_l(x,s)=\frac{1}{\omega_1}\left[\sum_{i=1}^{4}f_iC_i\exp(\lambda_i x)+D_2\exp(-x)\right], \tag{47}$$

Substituting Eqs. (46) and (47) into the transformed boundary conditions yields

$$\sum_{i=1}^{4}f_iC_i\lambda_i=D_2, \tag{48.a}$$

$$\sum_{i=1}^{4}f_iC_i\exp(\lambda_i a)=D_2\exp(-a), \tag{48.b}$$

$$\sum_{i=1}^{4}C_id_i=D_3, \tag{48.c}$$

$$\sum_{i=1}^{4}C_i\exp(\lambda_i a)=D_1\exp(-a), \tag{48.d}$$

where the coefficients C_i, $i=1,2,3,$ can be obtained by solving Eq. (48.a)-(48.d).

Substituting Eqs. (46) and (47) into Eq. (42) yields

$$\bar{\theta}_e(x,s)=\frac{1}{\Omega_4}\left[\sum_{i=1}^{4}g_iC_i\exp(\lambda_i x)+D_4\exp(-x)\right]. \tag{49}$$

From Eqs. (29), (46) and (41), we can get the following expression for the transformed stress:

$$\bar{\sigma}_{xx}=\frac{1}{\omega_1}\left[\sum_{i=1}^{4}d_iC_i\exp(\lambda_i x)-D_3\exp(-x)\right], \tag{50}$$

[see Appendix (B)].

Those complete the solution of ultrafast fractional thermal problem in the Laplace transform domain.

4. Inversion of Laplace transforms

In order to invert the Laplace transform in the above equations, we adopt a numerical inversion method based on a Fourier series expansion [38]. In this method, the inversion of Laplace transforms for the function $\bar{g}(s)$ is approximated by the relation:

$$g(t)=\frac{e^{\chi t}}{t_1}\left[\tfrac{1}{2}\bar{g}(\chi)+\mathrm{Re}\left(\sum_{k=1}^{\infty}e^{i\,k\,\pi t/t_1}\,\bar{g}(\chi+i\,k\,\pi/t_1)\right)\right]. \tag{51}$$

For numerical purposes this is approximated by the function

$$g_N(t)=\frac{e^{\chi t}}{t_1}\left[\frac{1}{2}\bar{g}(\chi)+\mathrm{Re}\left(\sum_{k=1}^{N}e^{i k \pi t/t_1}\,\bar{g}(\chi+i k\pi/t_1)\right)\right],\quad 0\le t\le 2t_1, \tag{52}$$

where N is a sufficiently large integer representing the number of terms in the truncated infinite Fourier series. N must be chosen such that:

$$e^{\chi t}\,\mathrm{Re}\left[e^{i N \pi t/t_1}\,\bar{g}(\chi+i N\pi/t_1)\right]\le \varepsilon_1,$$

where ε_1 is a small positive number that corresponds to the degree of accuracy to be achieved. The parameter c is a positive free parameter that must be greater than the real parts of all singularities of $\bar{g}(s)$. The optimal choice of c was obtained according to the criteria described in [40].

6. Numerical results and discussions

In the present work, a gold material is subjected to femtosecond pulsed laser heating, the mechanics and thermo physical properties of the metal are as follows [8], [46] and [47]:

$\rho=1.93\times10^{3}\,\mathrm{kg/m^3}$, $\alpha_T=14.2\times10^{-6}\,\mathrm{K^{-1}}$, $k_e=315\,\mathrm{W/mK}$, $C_e=2.1\times10^{4}\,\mathrm{J/m^3K}$, $C_l=2.5\times10^{6}\,\mathrm{J/m^3K}$, $\lambda=138.46\ \mathrm{GPa}$, $\mu=26.37\,\mathrm{GPa}$, and $G=2.8\times10^{16}\,\mathrm{W/m^3K}$.

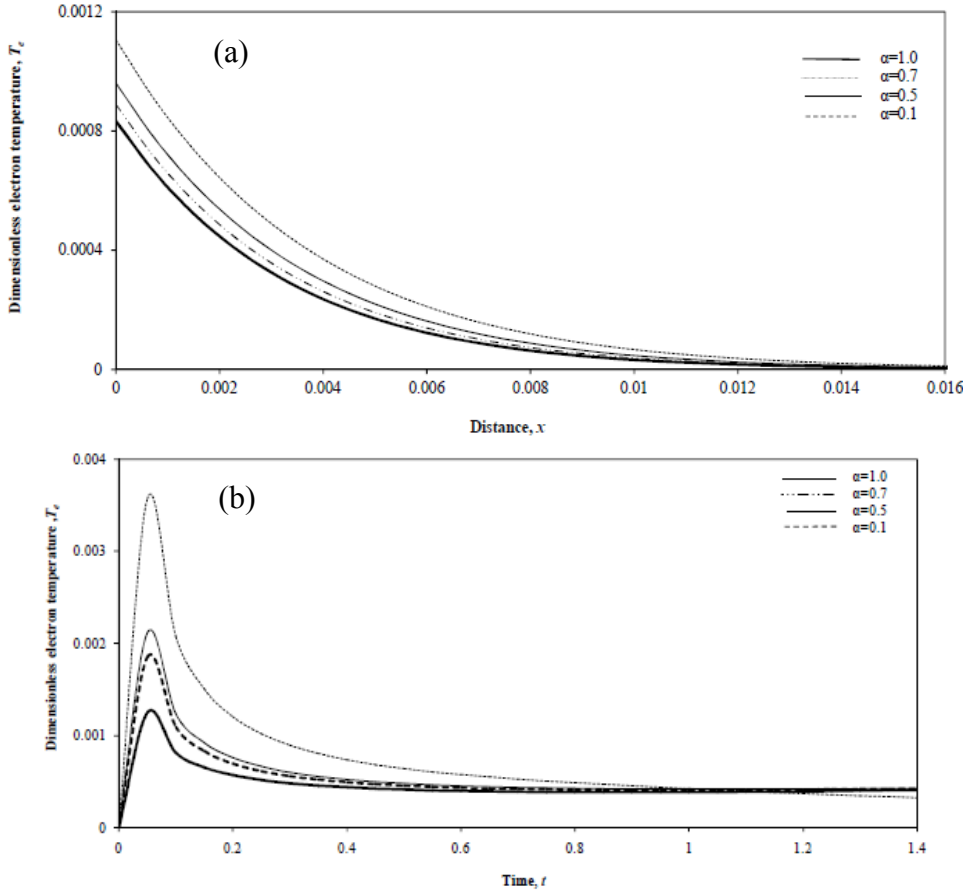

Fig. 1. The variation of the electron temperature T_e versus
(a) distance x for different values of parameter α at τ_e =0.02 and t=0.5, and
(b) time t for different values of parameter α at τ_e =0.02 and x=0.3.

The time duration and the energy intensity of the laser pulse are $t_p = 100$ fs and $J_0 = 13.4$ Watt / m^2, respectively. The absorptive depth of the heat energy is $x_0 = 15.3$ nm, and the rejectivity of the irradiated surface is $R = 0.93$ [8]. The ambient temperature is assumed to be room temperature, that is $T_0 = 300$ K.

The dimensionless electron temperatures on the front surfaces of metal at different values of fractional parameter α are shown in Figs 1.

Figure 1(a) shows the calculated electron temperature distribution versus distance *x* at different values of fractional parameter α. Figure 1(b) shows the calculated electron temperature distribution versus time *t* for different values of fractional parameter α. For any value of α, it appears that the electron temperature increases rapidly before it reaches a peak value and then decreases to nearly zero as time progresses because the absorbed laser energy is less than the sum of the energy transferring from the electrons to the lattice and the heat conducting into the deeper part of the electrons. It is interesting to observe that the variation of the electron temperature closely follows the temporal shape of the laser pulse. This is due to the mechanism of two-step heat conduction by which the heat energy of the laser pulse is first absorbed by electrons and then transferred to lattices. It is seen also that the electron temperatures for all value of $0 < \alpha \le 1$, reach peak values at the same time, namely, $t = 0.552$ and the peak value at $\alpha = 1$, is lower than that of the modification fractional model as $0 < \alpha < 1$.

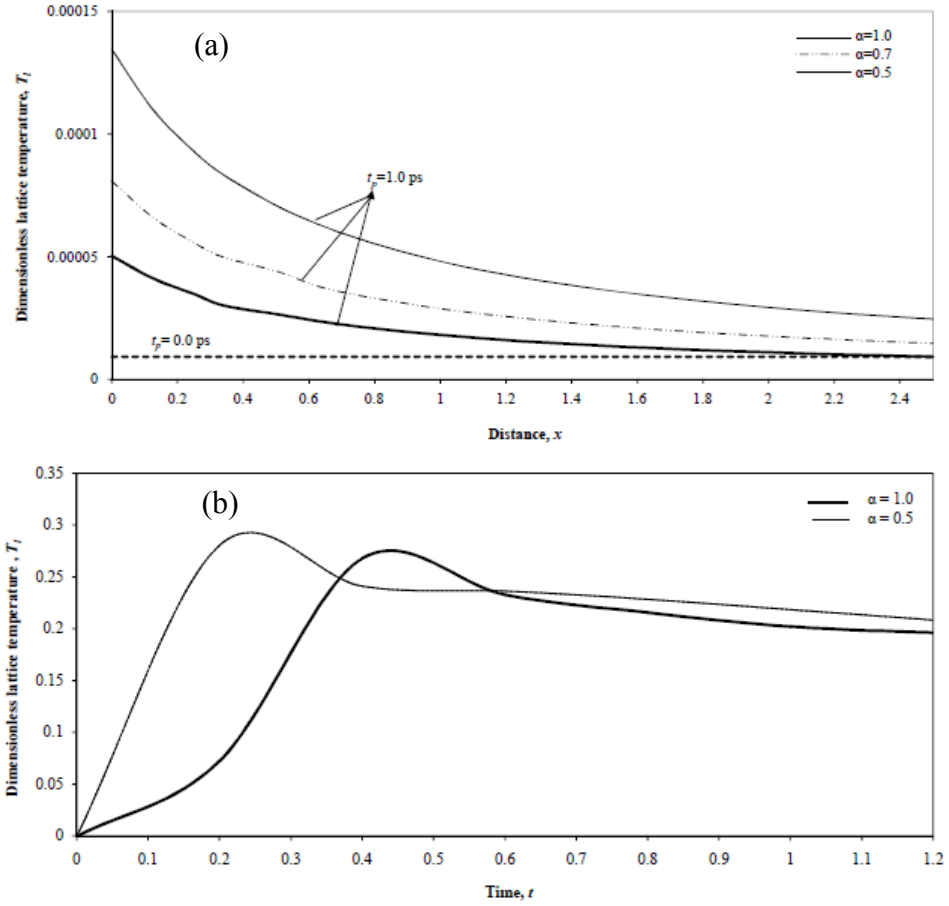

Fig. 2. The variation of lattice temperature T_l versus
(a) distance *x* for different values of parameter α at τ_e =0.02 and *t*=0.5, and
(b) time *t* for different values of parameter α at τ_e =0.02 and *x*=0.3.

Figure 2(a) shows the calculated lattice temperature distribution at different value of fractional parameter α. Figure 2(b) shows the lattice temperatures of the front surfaces of metal versus time t at different values of fractional parameter α. It is shown that the lattice temperature on the front surface increases rapidly before it reaches a peak value and then decays gradually as time proceeds. The peak value of it at $\alpha = 0.5$ is higher than that at $\alpha = 1$.

By comparing Fig. 1(b) with Fig. 2(b), for fixed both thermal relaxation time τ_e and $0 < \alpha \leq 1$ we notice that:

- The lattice temperature distribution is unlike the electron temperature, the maximum lattice temperature occurs at the front surface which is much lower than the maximum electron temperature, and it rises much slower than the electron temperature. This is due to the fact that the heat capacity of the metal lattice is about two orders of magnitude larger than that of the electrons [8].
- A large difference between the electron and lattice temperatures is observed, which indicates that the early stage of ultrafast laser heating is a non equilibrium process. The reason for this difference is that a portion of the energy is conducted away by the electron gas before the electrons and the lattice reach thermal equilibrium, thereby resulting in a lower lattice temperature increase. Also, it takes some time for energy to be transferred from the electrons to the lattice [46].

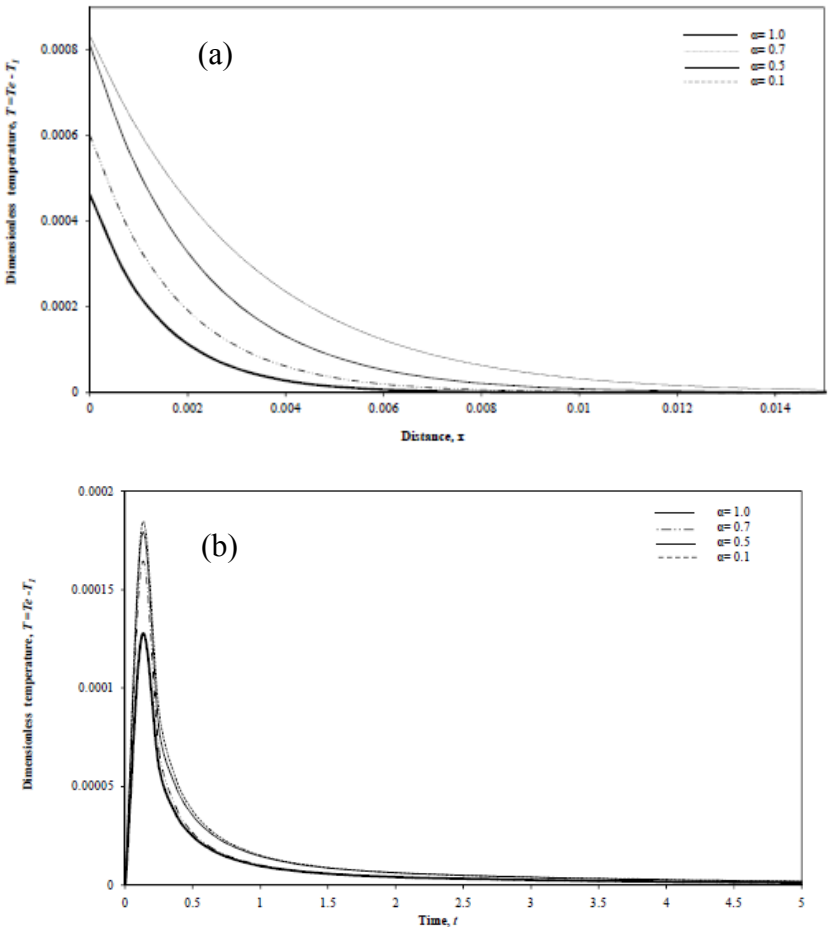

Fig. 3. The variation of equilibrium temperature $T = T_e - T_l$ versus (a) distance x for different values of parameter α at τ_e=0.02 and t=0.5, and (b) time t for different values of parameter α at τ_e=0.02 and x=0.3.

Figure 3(a) shows the variation of the equilibrium temperature $\theta = \theta_e = \theta_l$, with distance at different values of α for fixed thermal relaxation times.

Figure 3(b) shows the effect of fractional parameter on the equilibrium temperature distribution $\theta = \theta_e = \theta_l$, as we have noticed that the increasing of the value of the parameter α causes decreasing in the temperature and the temperature increment is continuous function, which means that the particles transport the heat to the other particles easily and this makes the decreasing rate of the temperature greater than the other ones, and the sharp temperature decreases marked by the arrows result from the thermal wave effect. This wave is quickly dissipated as it propagates into the material.

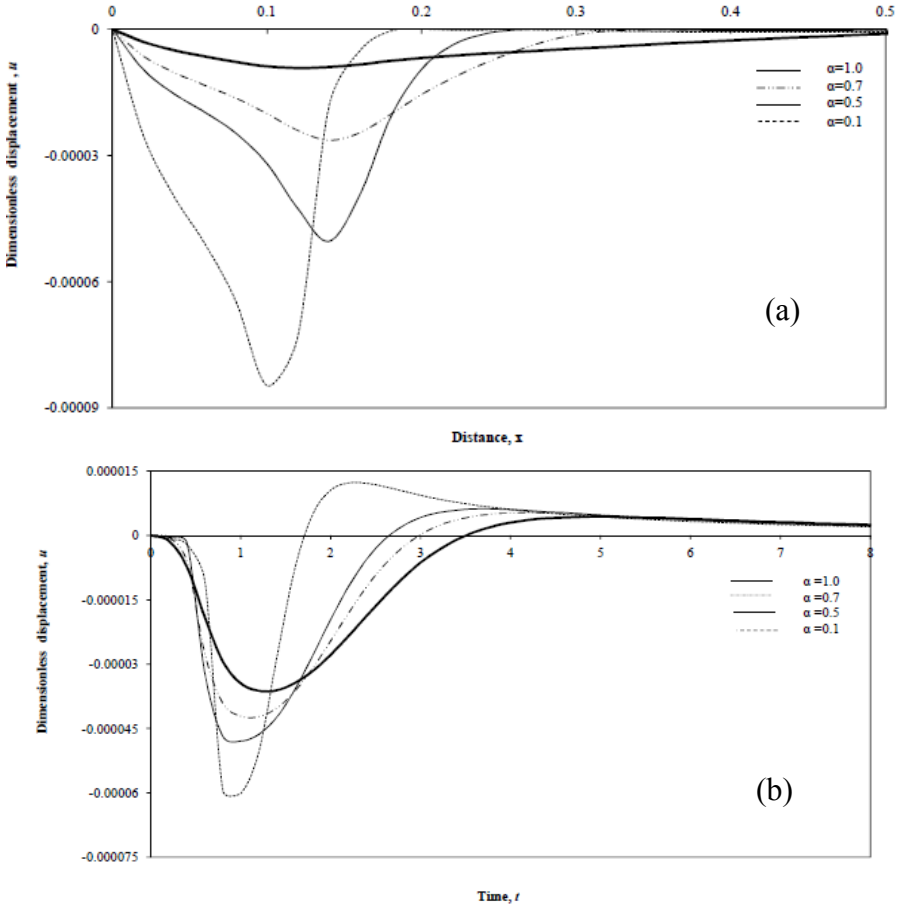

Fig. 4. The variation of displacement u versus
(a) distance x for different values of parameter α at τ_e =0.02 and t=0.5, and
(b) time t for different values of parameter α at τ_e =0.02 and x=0.3.

Figure 4(a) depicts the variation of thermal displacement u versus distance x, for time t = 0.6, the magnitude of the displacement first increases very rapidly with distance attains a maximum value and then gradually decreases to zero. In addition, when the value of the fractional order parameter α decreases, then the peak of the thermal displacement increases.

In Figure 4(b), to study the difference in the displacement history at different values of α, we calculated the displacement of metal at $\alpha = 0.1, 0.5, 0.7$. It is shown that the displacement in this case also vibrates, and the vibration period is longer than that at $\alpha = 1$. In addition, the absolute value of the equilibrium displacement and the vibration amplitude at $\alpha = 0.1$, is larger than those at $\alpha = 0.5$. The differences in the vibration period and magnitudes show the influences for α on the vibration behaviors very well.

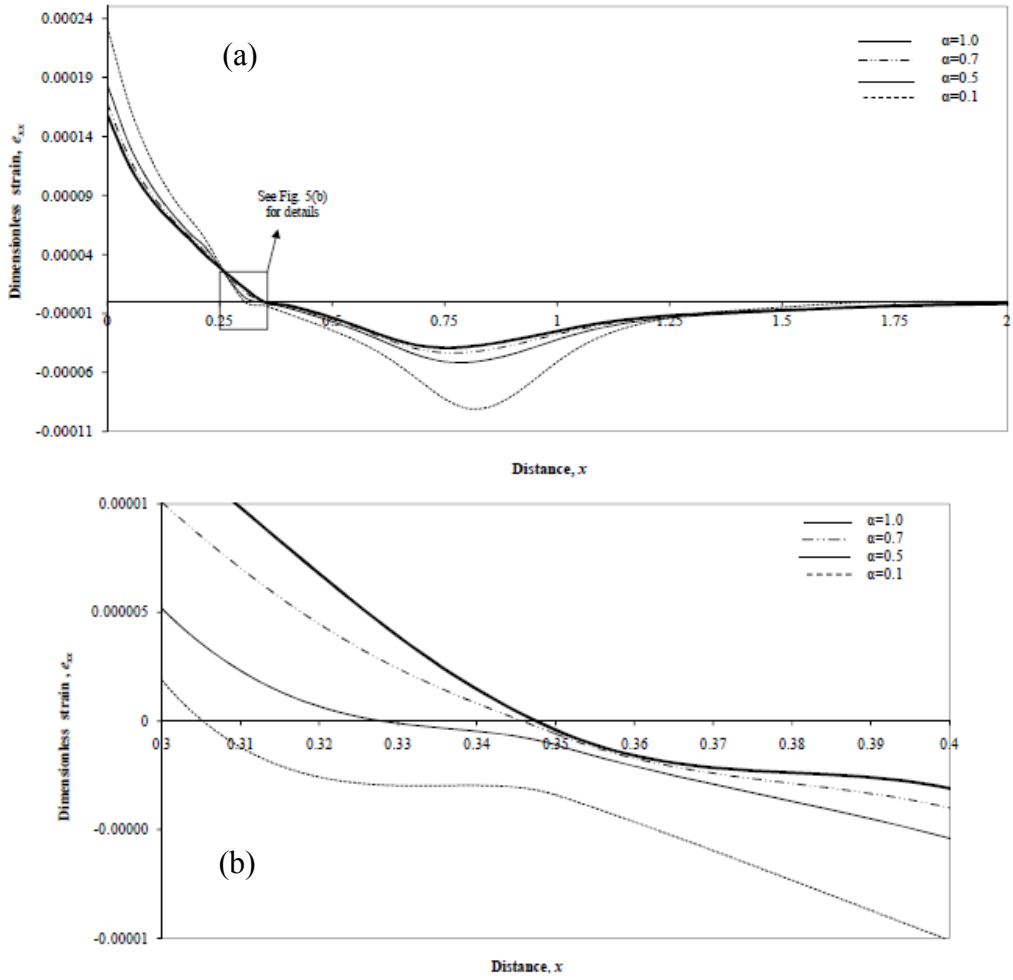

Fig. 5. The variation of strain e_{xx} versus distance $0.3<x<0.38$ for different values of parameter α at τ_e =0.02 and t=0.5.

Figure 5(a) gives the variation of thermal strain against distance x. The strain takes positive value in the range, $0 \le x \le 0.347$ ($\alpha = 1$), (see Fig. 5(b), for details) and the magnitude strain distribution after taking negative values goes on increasing, attains maximum values and then decreases slowly and finally vanishes.

Figure 6(a) represents variation of the spatial distributions of the stress versus distance at different fractional parameter value. Firstly, it increases to reach the peak value and also decreases with distance and finally goes to zero. The increment for α leads to decrease in its magnitude for fixed x.

Figure 6(b) shows how the stress wave at $\alpha = 0.5$ develops; the stress wave is completely developed.

Figures 5(c) and 6(c) show the effect of parameter α on strain and stress as the function of time.

From the above discussions, the presence of fractional order parameter α has a significant effect on the distribution of relevant variables.

7. Conclusions

• The main goal of the present work is to introduce a new mathematical model of two-step heat conduction with time fractional order α for fixed thermal relaxation (taking the memory effect into our account). The new model equations are employed to an isotropic

ultrafast thermoelastic material, as a new improvement and progress in the field of thermoelasticity. According to this theory, we have to construct a new classification to the materials according to its fractional parameter α where this parameter becomes a new indicator of its ability to conduct the heat in the material as affected on the electron, lattice and an equilibrium surface temperature value other than the thermal relaxation time such that a larger thermal relaxation causes a higher surface temperature increase. This is because a larger thermal relaxation time causes a slower heat propagation speed $\left(=\sqrt{\text{thermal diffusivity/ thermal relaxation time}}\right)$ as seen in figures. Therefore; more heat has accumulated near the surface.

- The effect of α on all the fields is also very much prominent, as the calculation results show that an ultrafast laser pulse at $\alpha=1,$ induces a stronger stress wave and stronger stress attenuation compared with $\alpha=0.5$. In addition, the peak values of the electron, lattice temperatures and the displacement are larger in a modified fractional model $(0<\alpha<1),$ as compared with the original model $(\alpha=1)$. Thus we can draw the conclusion that an ultrafast laser pulse induces a stronger thermo-mechanical response in a modified fractional model.

Appendix (A)

The parameters $\lambda_i, i=1,2,3,4$ represent the characteristic roots of Eq. (45) in our problem are given by

$$\lambda_j=\pm\sqrt{\frac{\Lambda_2+\sqrt{\Lambda_2^2-4\Lambda_1\Lambda_3}}{2\Lambda_1}},\ j=1,2, \qquad \lambda_j=\pm\sqrt{\frac{\Lambda_2-\sqrt{\Lambda_2^2-4\Lambda_1\Lambda_3}}{2\Lambda_1}},\ j=3,4,$$

where

$$\Lambda_1=\alpha\left[\Omega_4\Omega_5+s(\Omega_5+\Omega_3\Omega_6)\right],\ \Lambda_2=\Omega_4 s^3+(\Omega_5+\alpha\Omega_4+\Omega_3\Omega_6)s^2+(\Omega_5+\Omega_4\Omega_5+\Omega_3\Omega_6)s,$$

$$\Lambda_3=s^3(s+\Omega_4+1),\ \Lambda_4=\beta\Omega_4\Omega_6.$$

Appendix (B)

The relevant coefficients $D_i,\ f_i, d_i$ and $g_i, i=1,2,3,4$ of the problem used before in Eqs. (45)-(50) are given by

$$D_1=\frac{\Lambda_4}{\Lambda_1-\Lambda_2+\Lambda_3},\quad D_2=\omega_4-\omega_2 D_1+\omega_3 D_1, \qquad D_3=A_1\omega_1 D_1+A_2 T_0 D_2,$$

$$D_4=\frac{s+\Omega_4}{\omega_1}D_2+\Omega_3 D_1 s, \qquad f_i=b_2\lambda_i^3-b_3\lambda_i \text{ , and } g_i=\frac{s+\Omega_4}{\omega_1}f_i+\Omega_3 s\lambda_i .$$

Appendix (C)

The Laplace transform rule with the Caputo derivative which is defined as

$$L\{D_C^{\alpha}g(t)\}=\{s^{\alpha}\bar{g}(s)\}-\sum_{K=0}^{n-1}f^{\,k}(0^+)s^{\alpha-1-k},\quad n-1<\alpha<n.$$

Note that we use the Caputo fractional derivative omitting the index C. It should be noted that if initial conditions are properly taken into account.

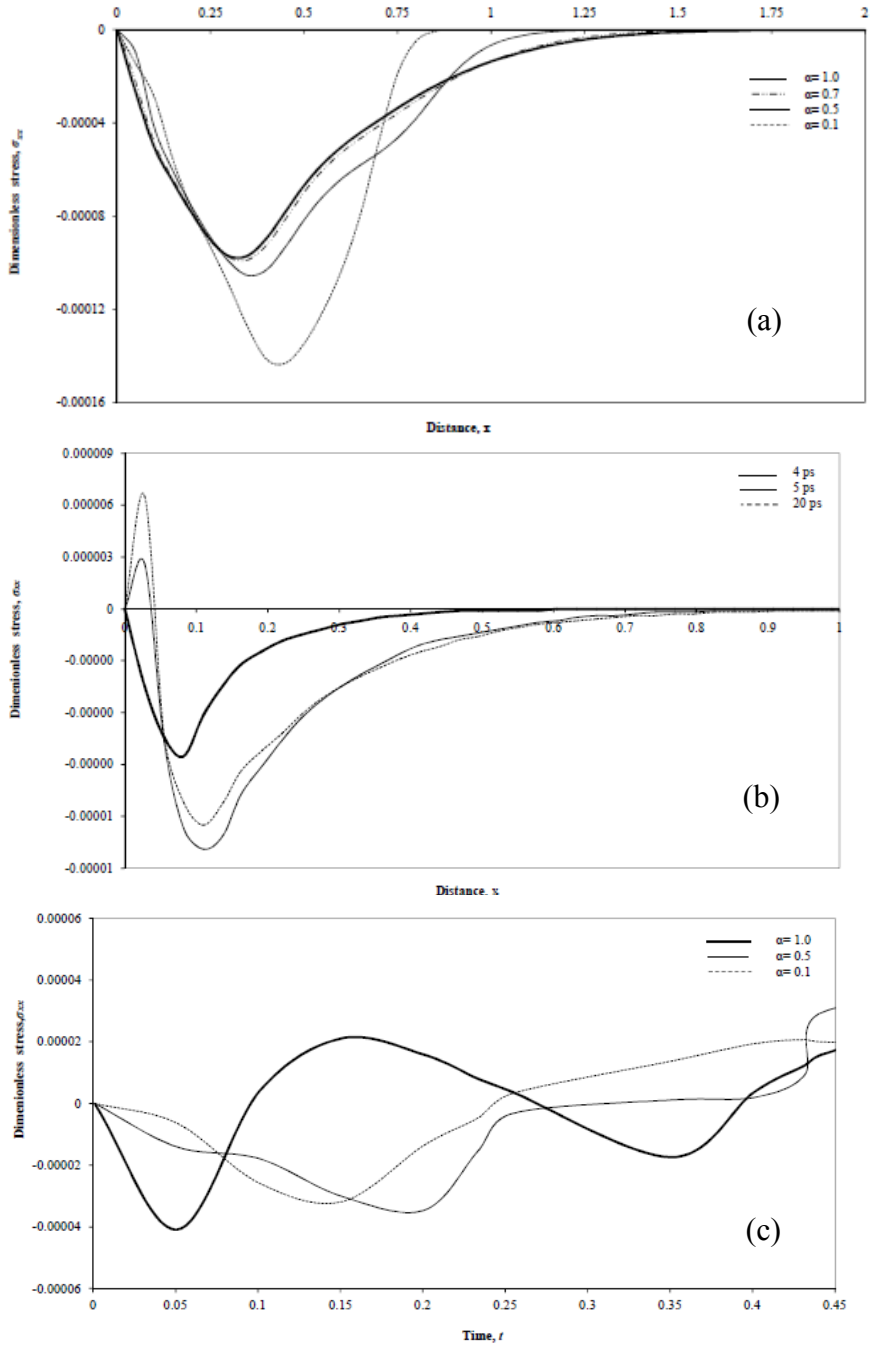

Fig. 6. The variation of stress σ_{xx} versus

(a) distance x for different values of parameter α at τ_e =0.02 and t=0.5,

(b) distance x for different time at $\alpha = 0.5$ and τ_e =0.02, and

(c) time t for different values of parameter α at τ_e =0.02 and x=0.3.

References

[1] S.I. Anisimov, B.L. Kapeliovich, T.L. Perel'man // *Journal of Experimental and Theoretical Physics* **39(2)** (1974) 375.

[2] J.K. Chen, J.E. Beraun, C.L. Tham // *International Journal of Engineering Science* **42** (2004) 793.

[3] M.N. Özişik, D.Y. Tzou // *Journal of Heat Transfer* **116(3)** (1994) 526.

[4] W.S. Kim, L.G. Hector Jr., M.N. Özisik // *Journal of Applied Physics* **68(11)** (1990) 5478.

[5] T.Q. Qiu, C.L. Tien // *Journal of Heat Transfer* **115(4)** (1993) 835.
[6] Yuxin Sun, Masumi Saka, Jing Li, Jialing Yang // *International Journal of Mechanical Sciences* **52** (2010) 1202.
[7] F. A. McDonald // *Applied Physics Letters* **56(3)** (1990) 230.
[8] J.K. Chen, J.E. Beraun, L.E. Grimes, D.Y. Tzou // *International Journal of Solids and Structures* **39(12)** (2002) 3199.
[9] M. Caputo // *Geophysical Journal of the Royal Astronomical Society* **13(5)** (1967) 529.
[10] I. Podlubny, *Fractional Differential Equations* (Academic Press, New York, 1999).
[11] F. Mainardi, R. Gorenflo // *Journal of Computational and Applied Mathematics* **118(1-2)** (2000) 283.
[12] R. Gorenflo, F. Mainardi, *Fractional Calculus: Integral and Differential Equations of Fractional Orders*, In: Fractals and Fractional Calculus in Continuum Mechanics ed. by A. Carpinteri, F. Mainardi (Springer Verlag, New York and Wien, 1997), p. 223.
[13] K.S. Miller, B. Ross, *An Introduction to the Fractional Integrals and Derivatives Theory and Applications* (John Wiley & Sons Inc., New York, 1993).
[14] S.G. Samko, A.A. Kilbas, O.I. Marichev, *Fractional Integrals and Derivatives Theory and Applications* (Gordon and Breach Science Publishers, Langhorne, PA, 1993).
[15] K.B. Oldham, J. Spanier, *The Fractional Calculus: Theory and Applications of Differentiation and Integration to Arbitrary Order* (Dover Books on Mathematics, New York, 2006).
[16] R. Hilfer, *Applications of Fraction Calculus in Physics* (World Scientific, Singapore, 2000).
[17] M. Caputo, F. Mainardi // *La Rivista del Nuovo Cimento* (Ser II) **1** (1971) 161.
[18] R.L. Bagley, P.J. Torvik // *Journal of Rheology* **27(3)** (1983) 201.
[19] RC. Koeller // *Journal of Applied Mechanics* **51** (1984) 299.
[20] Y.A. Rossikhin, M.V. Shitikova // *Applied Mechanics Reviews* **50** (1997) 15.
[21] S. Grimnes, O.G. Martinsen, *Bioimpedance and Bioelectricity Basics* (Academic Press, San Diego, CA, 2000).
[22] R.S. Lakes, *Viscoelastic Solids* (CRC Press, Boca Raton, FL, 1999).
[23] R.L. Magin // *Critical Reviews in Biomedical Engineering* **32** (2004) 1.
[24] R. Magin, *Fractional Calculus in Bioengineering* (Begell House Inc., Redding, CT, 2006).
[25] Y.Z. Povstenko // *Journal of Thermal Stresses* **28** (2005) 83.
[26] Y.Z. Povstenko // *Mechanics Research Communications* **37(4)** (2010) 436.
[27] H.H. Sherief, A.M.A. El-Sayed, A.M. Abd El-Latief // *International Journal of Solids and Structures* **47(2)** (2010) 269.
[28] H. Youssef // *Journal of Heat Transfer* **132(6)** (2010) 061301.
[29] M.A. Ezzat // *Physica B: Condensed Matter* **405** (2010) 4188.
[30] M.A. Ezzat // *Physica B: Condensed Matter* **406** (2011) 30.
[31] G. Jumarie // *Computers & Mathematics with Applications* **59** (2010) 1142.
[32] A.S. El-Karamany, M.A. Ezzat // *Journal of Thermal Stresses* **34** (2011) 264.
[33] A.S. El-Karamany, M.A. Ezzat // *Mathematics and Mechanics of Solids* **16(3)** (2011) 334.
[34] M.A. Ezzat, M.A. Fayik // *Journal of Thermal Stresses* **34** (2011) 851.
[35] M.A. Ezzat, A.S. El-Karamany // *Canadian Journal of Physics* **89(3)** (2011) 311.
[36] M.A. Ezzat, A.S. El-Karamany // *ZAMP, Zeitschrift für angewandte Mathematik und Physik* **62(5)** (2011) 937.
[37] M.A. Ezzat // *Canadian Journal of Physics* **86(11)** (2008) 1241.
[38] G. Honig, U. Hirdes // *Journal of Computational and Applied Mathematics* **10(1)** (1984) 113.

[39] J. Hohlfeld, S.-S. Wellershoff, J. Güdde, U. Conrad, V. Jähnke, E. Matthias // *Chemical Physics* **251(1-3)** (2000) 237.
[40] G. L. Eesley // *Physical Review B* **33(4)** (1986) 2144.
[41] H.E. Elsayed-Ali, T.B. Norris, M.A. Pessot, G.A. Mourou // *Physical Review Letters* **58(12)** (1987) 1212.
[42] P.G. Klemens, R.K. Williams // *International Materials Reviews* **31(1)** (1986) 197.
[43] L. Spitzer Jr., *Physics of Fully Ionized Gases* (John Wiley, New York, 1962).
[44] L. Spitzer, Jr., R. Härm // *Physical Review* **89(5)** (1953) 977.
[45] D.W. Tang, N. Araki // *International Journal of Heat and Mass Transfer* **42** *(*1999) 855.
[46] X. Wang, X. Xu // *Journal of Thermal Stresses* **25** (2002) 457.
[47] J.K. Chen, J.E. Beraun // *Numerical Heat Transfer, Part A: Applications* 40 (2001) 1.